THE JOURNAL OF PHYSICAL CHEMISTRY A

Article

pubs.acs.org/JPCA

Nonempirical Anharmonic Vibrational Perturbation Theory Applied to Biomolecules: Free-Base Porphin

Sergey V. Krasnoshchekov* and Nikolay F. Stepanov

Lomonosov Moscow State University, Leninskiye Gory, 119991 Moscow, Russian Federation

Supporting Information

ABSTRACT: Anharmonic vibrational frequencies and intensities (infrared and Raman) of an isolated free-base porphin molecule are predicted from the quantum mechanical (QM) geometry, the "semi-diagonal" quartic force field, and dipole moment and polarizability surfaces. The second-order vibrational perturbation theory plus the numerical diagonalization of the Hamiltonian matrix containing off-diagonal Fermi and Darling–Dennison resonance couplings (VPT2+*WK*) was used. The QM calculations were carried out with the Becke–Lee–Yang–Parr composite exchange–correlation functional (B3LYP) and with the 6-31+G(d,p) basis set. The harmonic force field for the equilibrium configuration was transformed into nonredundant local symmetry internal coordinates, and normal coordinates were defined. The semi-diagonal quartic rectilinear normal coordinate potential energy surface (PES), as well as the cubic surfaces of dipole moment (p) and polarizability (α) components, needed for the VPT2+*WK* calculation, were constructed by a five-point finite differentiation of Hessians (for PES) and of the values and first derivatives of p and α. They were obtained at the point of equilibrium and for 432 displaced configurations. This theoretical approach provides very good agreement between the predicted and experimental frequencies and intensities. However, the favorable result can be partly attributed to error cancellation within the B3LYP/6-31+G(d,p) QM model, as observed in earlier studies. Reassignments of some observed bands are proposed.

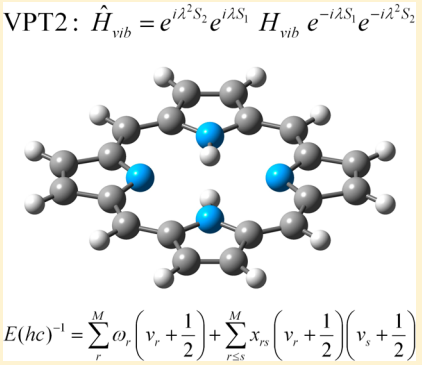

1. INTRODUCTION

Porphin is the prototype of porphyrins, an important class of bioorganic molecules that form framework groups of many proteins, such as hemoproteins (e.g., hemoglobin), cytochromes, and phtalocyanines.[1,2] Porphin's two protons from N–H bonds can be substituted by divalent cations of many metals, magnesium, zinc, iron, cobalt, nickel, copper, chromium, manganese, silver, palladium, and so forth, to form a class of biologically active and important derivatives called metalloporphyrins. Metalloporphyrins with heme groups are very important for biological processes functioning, in particular, in photosynthesis, oxygen transport, and oxidation–reduction mechanisms. Insight into the structure and vibrations of metalloporphyrins requires a thorough study of the parent molecule. The spectroscopic characterization of this class of molecules has considerable interest to a large community of chemists and biochemists.

Both porphin and metalloporphyrins have received much attention in experimental studies of structure and spectra, as well as theoretical normal coordinate analyses in the last few decades.[3−31] A high-symmetry point group D_{2h} and plentiful experimental data on porphin support the study of its vibrations. Porphin in the solid state and dispersed in a noble gas matrix was studied by means of infrared (IR) spectra,[4−8] resonance Raman (RR) spectra,[9−11] nonresonance Raman spectra,[12] and luminescence/phosphorescence spectra.[13−15] A measurement of inelastic neutron scattering (INS) spectra for porphin permitted observation of many previously unknown fundamental vibrational bands, including both IR- and Raman-inactive A_u transitions.[16]

Early studies of normal coordinates and the force field for porphin depended on solving the inverse vibrational problem.[17−29] The theoretical electronic quantum mechanical (QM) studies of porphin received a boost with the introduction of the density functional theory (DFT). A number of porphin studies employing the DFT-B3LYP functional has demonstrated that this level of theory produces a sufficiently accurate description of the vibrations of porphin following an empirical adjustment of the harmonic force field.[12,16,20,21,23−26]

Predicted harmonic frequencies usually do not match the experimentally observed vibrational band centers for two main reasons. First, anharmonic shifts can be large, even over 100 cm^{-1}. Second, only a few QM models [such as CCSD(T), for instance] produce molecular geometries and potential energy surfaces (PESs) of sufficient quality. These models are inapplicable to molecules of the size of porphin at a reasonable cost. The previous studies inevitably used a phenomenological tool—scaling of the harmonic force field—to achieve an acceptable agreement between calculated and observed fundamental frequencies.[12,20,21,23−26] The scaled quantum

Special Issue: 25th Austin Symposium on Molecular Structure and Dynamics

Received: July 31, 2014
Revised: October 31, 2014
Published: October 31, 2014

dx.doi.org/10.1021/jp5077092 | J. Phys. Chem. A 2015, 119, 1616–1627

mechanical (SQM) force field is a well-established technique, often associated with Peter Pulay.[32,33] The scaling technique is based on the more-or-less regular character of anharmonic shifts and QM model deficiencies. Applying sets of scaling factors obtained for harmonic force fields of smaller molecules or molecules of similar structure to a new molecule effectively absorbs regular shifts of frequencies and achieves an acceptable reproduction of observed data.

The empirical character of the SQM force field technique is only part of the problem. The other complication is that the anharmonic character of molecular vibrations leads to substantial coupling between normal modes, which results in Fermi resonances (FRs), mode mixing, and intensity borrowing.[34−38] These widely observed effects cannot be described by a harmonic model; a more sophisticated anharmonic model must be employed. In some cases, nonfundamental transitions can have substantial intensities that cannot be described within a harmonic model.

All previous vibrational analyses of porphin were performed in the framework of the so-called "double-harmonic approximation", that is, using quadratic force constants and first derivatives from the dipole moment and polarizability tensor components. Using modern capabilities of quantum chemistry (e.g., DFT), an anharmonic model of molecular vibrations, and adequate computer resources enables more advanced studies, based, for example, on the second-order vibrational perturbation theory (VPT2).[34−43]

It may sound surprising, but the application of the well-established VPT2 method of computing anharmonic vibrations to the large porphin molecule does not meet any obstacles that cannot be overcome by an appropriately chosen computational technique. First, the force field required for VPT2 can be reduced to the so-called "semi-diagonal" version, where the number of different modes participating in quartic force constants is limited to three. In other words, force constants of the form ϕ_{rstu} are not computed. This approximation sacrifices the important type of 11−11 Darling−Dennison (D−D) resonance but preserves the 1−1 type. However, these 11−11 perturbations do not directly affect fundamentals. Consequently, only single and double differentiation of analytic Hessians along each of M = 108 normal modes of porphin is required. In addition to computing the equilibrium structure, the minimum task is to evaluate Hessians in only $2 \times M$ displaced configurations. The calculation of the full quartic force field would require $2 \times M \times (M - 1)$ additional evaluations of harmonic force constants that would be far from practical. For the B3LYP/6-31G+(d,p) QM model, which has demonstrated good results in a number of studies,[44,45] the computational time for obtaining a Hessian for each configuration is quite reasonable, and such evaluations can be organized in parallel. Both the potential energy and the molecular properties surfaces can be efficiently kept in computer memory in a compact form without repeating equivalent derivatives.

Second, the calculation of the anharmonic constants (x) as well as Fermi (W) and D−D (K) resonance coupling constants can be efficiently accomplished using closed expressions.[46−50] The final stage of the calculation (designated by adding the suffix +*WK* to VPT2) requires evaluation of matrix elements for the resonance terms of the Hamiltonian, using an appropriate set of harmonic oscillator basis functions. If the maximum excitation of these basis functions is restricted to two quanta, which covers first overtones and binary combination states, then the size of such a basis set for porphin is on the order of 6000, which is acceptable. The diagonalization of the Hamiltonian matrix containing resonance couplings produces a final set of anharmonic frequencies and the matrix of eigenvectors that are used for mixing intensities calculated for "pure" fundamentals, overtones, and combinations bands. As a result, a simulated spectrum with a realistic picture of the intensity distribution among "bright" and "dark" states can be obtained.

The density of transitions for molecules of the size of porphin is quite high, especially in the important region of C−H stretching vibrations (about 3000 cm^{-1}). Thus, it is very useful to be able to predict not only the frequencies of transitions but also their intensities (IR and Raman). The analytical expressions for anharmonic intensities of both fundamental (0−1) and two-quanta transitions (0−11, 0−2) are available in the literature for IR spectra[51−60] and Raman spectra.[45,56,60−63]

The primary goal of this work is obtaining a nonempirical theoretical prediction of the anharmonic IR and Raman spectra of porphin and taking a step forward in developing a methodology for predicting vibrational spectra of large biologically important molecules without any involvement of empirical information drawn from the spectrum of the target or related molecules. Such a prediction of spectra can be accomplished in a "black-box virtual spectrometer" style[60] to ensure easy access to computational facilities by biochemists.

2. THEORETICAL BACKGROUND

In this section, we briefly review the main theoretical considerations needed for understanding the VPT2 method applied to modeling the anharmonic vibrational spectra of porphin.

2.1. Hamiltonian and the Second-Order Vibrational Perturbation Theory (VPT2+*WK*). The traditional implementation of the VPT2 employs a Watson Hamiltonian of a molecule with M degrees of vibrational freedom expanded in powers of rectilinear dimensionless normal coordinates $q_r = Q_r[4\pi^2c^2\omega_r(hc)^{-1}]^{1/2}$, where ω_r is a harmonic frequency and Q_r is Wilson's normal coordinate. The Hamiltonian operator $H = T + V$ grouped by 0, 1, and 2 orders of perturbation theory is represented by

$$\begin{aligned} H &= T + V \\ &= \left[\frac{1}{2}\sum_{r}^{M}\omega_r(p_r^2 + q_r^2)\right] + \left[\frac{1}{6}\sum_{r}^{M}\sum_{s}^{M}\sum_{t}^{M}\phi_{rst}q_rq_sq_t\right] \\ &\quad + \left[\frac{1}{24}\sum_{r}^{M}\sum_{s}^{M}\sum_{t}^{M}\sum_{u}^{M}\phi_{rstu}q_rq_sq_tq_u \right. \\ &\quad \left. + \sum_{\alpha=x,y,z}B_e^{\alpha}\left(\sum_{r}^{M}\sum_{s}^{M}\sum_{t}^{M}\sum_{u}^{M}\zeta_{rs}^{\alpha}\zeta_{tu}^{\alpha}\left(\frac{\omega_s}{\omega_r}\right)^{1/2}\left(\frac{\omega_u}{\omega_t}\right)^{1/2}q_rp_sq_tp_u\right)\right] \end{aligned} \tag{2.1}$$

where ϕ_{rst},ϕ_{rstu} are force constants, B_e^{α} are equilibrium rotational constants (both in cm^{-1} units), and ζ_{rs}^{α} are Coriolis coupling constants.

After reduction of the Hamiltonian (eq 2.1) to the desired quasi-diagonal form $\hat{H}^{(2)}$ using canonical van Vleck perturbation theory in second order[34−38] and integration of $\hat{H}^{(2)}$ with the zero-order harmonic oscillator basis functions $E(\overline{v}) = hc\langle\Phi(\overline{v})|\hat{H}^{(2)}|\Phi(\overline{v})\rangle$, one obtains the following analytic

dx.doi.org/10.1021/jp5077092 | J. Phys. Chem. A 2015, 119, 1616−1627

expression for vibrational terms as a function of harmonic frequencies and anharmonic constants G_0, x_{rs}

$$E(hc)^{-1} = G_0 + \sum_{r}^{M} \omega_r\left(\nu_r + \frac{1}{2}\right) + \sum_{r\le s}^{M} x_{rs}\left(\nu_r + \frac{1}{2}\right)\left(\nu_s + \frac{1}{2}\right) \tag{2.2}$$

as well as expressions for Fermi (W) and D−D (K) resonance off-diagonal constants.[46−50] In the final variational stage (denoted by $+WK$ addition to the VPT2 abbreviation), a suitable set of zero-order harmonic oscillator basis functions is chosen to account for first- and second-order resonance couplings. This set is usually much smaller than would have been used in a full variational treatment of the vibrational Schrödinger equation. The eigenvalues obtained after numerical diagonalization are the final anharmonic energy terms, while the eigenvectors describe mixing of the zero-order states. The eigenvectors are further used for obtaining the final transition moments of resonant vibrational levels as linear combinations of deperturbed (DP) values.

2.2. IR Intensities. Because the density of an anharmonic vibrational spectrum grows rapidly with the size of the molecule and an increase of excitation energy, a great help for interpreting spectra can be gained from an anharmonic calculation of IR and Raman intensities.[45,51−63] Close-lying anharmonic vibrational states can be strongly coupled due to resonance interactions, and an accompanying intensity redistribution can take place, which cannot be described in the framework of the conventional harmonic model. In addition, anharmonic terms in the dipole moment and polarizability tensor components must be accounted for.

As was shown in early fundamental studies of the VPT2 theory,[64,65] transition matrix elements for the anharmonic (i.e., nonlinear in coordinates q_r) operator ρ of a molecular property (such as Cartesian components of the dipole moment, polarizability tensor, etc.) can be approximated by matrix elements of the double contact-transformed operators with zero-order harmonic wave functions, that is

$$\langle\Phi^{(a)}|\rho|\Phi^{(b)}\rangle = \langle\Phi_0^{(a)}|U\rho U^{-1}|\Phi_0^{(b)}\rangle = \langle\Phi_0^{(a)}|\mathrm{P}|\Phi_0^{(b)}\rangle \tag{2.3}$$

where U is the unitary operator representing a double canonical transformation reducing the Hamiltonian to the quasi-diagonal form.

For this purpose, for example, the effective dipole moment operator $\mu_\alpha = \mu_\alpha(q)$, $\alpha = x,y,z$, must be expanded in powers of normal coordinates and duly arranged by orders of perturbation theory

$$\mu_\alpha(q) = \left[\mu_\alpha^{\,0} + \sum_r \left(\frac{\partial\mu_\alpha}{\partial q_r}\right)_0 q_r\right] + \left[\frac{1}{2}\sum_{rs}\left(\frac{\partial^2\mu_\alpha}{\partial q_r\partial q_s}\right)_0 q_r q_s\right] + \left[\frac{1}{6}\sum_{rst}\left(\frac{\partial^3\mu_\alpha}{\partial q_r\partial q_s\partial q_t}\right)_0 q_r q_s q_t\right] + \ldots \tag{2.4}$$

At the second order, the transformed dipole moment operator M_α has the following form[52]

$$\mathrm{M}_\alpha = \left(\mu_\alpha^{(0)} + \mathrm{i}[S_1, \mu_\alpha^{(0)}] - \frac{1}{2}[S_1, [S_1, \mu_\alpha^{(0)}]] + \mathrm{i}[S_2, \mu_\alpha^{(0)}]\right) + (\mu_\alpha^{(1)} + \mathrm{i}[S_1, \mu_\alpha^{(1)}]) + \mu_\alpha^{(2)} \tag{2.5}$$

where $\mu_\alpha^{(k)}$ is the kth perturbation of the dipole moment operator and operator S_k is the generator of the kth contact transformation. Once the explicit expression of M_α is known, it is easy to evaluate the line strength $S^{(ab)}$ of the dipole $a \leftarrow b$ transition, which is given by

$$S^{(ab)} = \sum_\alpha |\langle\Phi_0^{(a)}|\mathrm{M}_\alpha|\Phi_0^{(b)}\rangle|^2 \tag{2.6}$$

Analytic expressions for the line strengths of fundamentals, first overtones, and binary combination transitions have been derived and are available in the literature.[51−60]

The integral absorption coefficient of electric dipole moment $\alpha \leftarrow b$ for the Boltzmann distribution of molecules at absolute temperature T is given by the following formula[38]

$$I^{(ab)} = \frac{8\pi^3 N_\mathrm{A}}{3hcQ}\nu^{(ab)}S^{(ab)}\left[\exp\left(-\frac{E^{(b)}}{kT}\right) - \exp\left(-\frac{E^{(a)}}{kT}\right)\right] \tag{2.7}$$

where N_A is the Avogadro number, k is the Boltzmann constant, $\nu^{(ab)}$ is the $\alpha \leftarrow b$ transition wavenumber, and Q is the vibrational partition function.

2.3. Raman Intensities. The same theory is applicable to the tensor components of the polarizability operator $\alpha_{\xi\zeta}(q)$, where $\xi,\zeta = x,y,z$, as long as these components are expanded in a Taylor series in the same way as eq 2.4.[45,56,61−63] In the Raman scattering vibrational spectra (RS), a differential cross section of scattering can be used as a quantity characterizing the intensity of the jth band (in units of 10^{-48} cm^2/sr)

$$\frac{\partial\sigma_j}{\partial\Omega} = \frac{(2\pi)^4}{45}(\nu_0 - \nu_j)^4\left[1 - \exp\left(-\frac{hc}{kT}\nu_j\right)\right]^{-1}\frac{hc}{8\pi^2c^2\nu_j}S_{\mathrm{RS}}(\nu_j) \tag{2.8}$$

Here, $(\partial\sigma_j/\partial\Omega)$ is the Raman scattering cross section; ν_0 is the frequency of the excitation line; h, c, and k are universal constants; T is the absolute temperature; and Ω is the solid angle at which light is recorded. The quantity $S_{\mathrm{RS}}(\nu_j) = 45\bar{\alpha}_j^2 + 7\gamma_j^2$ is called the coefficient of Raman scattering activity, in which invariants $\bar{\alpha}_j^2$, γ_j^2 (mean polarizability and anisotropy) have the form[66]

$$\bar{\alpha}_j^2 = \frac{1}{9}[\langle\Phi^{(a)}|\alpha_{xx}|\Phi^{(b)}\rangle + \langle\Phi^{(a)}|\alpha_{yy}|\Phi^{(b)}\rangle + \langle\Phi^{(a)}|\alpha_{zz}|\Phi^{(b)}\rangle]^2 \tag{2.9}$$

$$\begin{aligned}\gamma_j^2 = {} & \frac{1}{2}[\langle\Phi^{(a)}|\alpha_{xx}|\Phi^{(b)}\rangle - \langle\Phi^{(a)}|\alpha_{yy}|\Phi^{(b)}\rangle]^2 \\ & + \frac{1}{2}[\langle\Phi^{(a)}|\alpha_{yy}|\Phi^{(b)}\rangle - \langle\Phi^{(a)}|\alpha_{zz}|\Phi^{(b)}\rangle]^2 \\ & + \frac{1}{2}[\langle\Phi^{(a)}|\alpha_{zz}|\Phi^{(b)}\rangle - \langle\Phi^{(a)}|\alpha_{xx}|\Phi^{(b)}\rangle]^2 \\ & + 3[\langle\Phi^{(a)}|\alpha_{xy}|\Phi^{(b)}\rangle^2 + \langle\Phi^{(a)}|\alpha_{yz}|\Phi^{(b)}\rangle^2 + \langle\Phi^{(a)}|\alpha_{zx}|\Phi^{(b)}\rangle^2]\end{aligned} \tag{2.10}$$

If the operator $\alpha_{\xi\zeta}(q)$ is subjected to a transformation eq 2.5, one can obtain a transformed operator of the polarizability component $\mathrm{A}_{\xi\zeta}$, whose matrix elements in the basis of the harmonic oscillator's eigenfunctions are equal to the matrix elements of the initial operator for anharmonic functions

$$\langle\Phi^{(a)}|\alpha_{\xi\zeta}|\Phi^{(b)}\rangle = \langle\Phi_0^{(a)}|\mathrm{A}_{\xi\zeta}|\Phi_0^{(b)}\rangle \tag{2.11}$$

It should be noted that it can be convenient to calculate the absolute normalized differential cross section of scattering,

dx.doi.org/10.1021/jp5077092 | J. Phys. Chem. A 2015, 119, 1616−1627

which is defined by moving the factor $(\nu_0 - \nu_j)^4$ in eq 2.8 to the left side and therefore avoiding dependence on the frequency of the excitation line.

In order to calculate the values for the anharmonic Raman intensities of overtones and combination transitions, the analogous formulas as used for IR intensities are applicable too.[45,60,63]

3. CALCULATION DETAILS

3.1. Porphin Symmetry, Geometry, and Internal Coordinates. The free porphin molecule belongs to the symmetry point group D_{2h}, and its normal modes can be classified as follows: $19A_g$ (in-plane, Raman-active), $8A_u$ (out-of-plane, IR- and Raman-inactive), $18B_{1g}$ (in-plane, Raman-active), $10B_{1u}$ (out-of-plane, IR-active), $9B_{2g}$ (out-of-plane, Raman-active), $18B_{2u}$ (in-plane, IR-active), $8B_{3g}$ (out-of-plane, Raman-active), and $18B_{3u}$ (in-plane, IR-active). Thus, mutual exclusion applies to IR and Raman activities for this centrosymmetric molecule.

The porphin molecular properties such as the equilibrium geometry, harmonic force constants, dipole moment vector components and their first derivatives, as well as polarizability tensor components in Cartesian coordinates were computed with the aid of QM method DFT-B3LYP and the basis set 6-31G+(d,p). The choice of this QM method and basis set was motivated by the success of this combination for a number of large molecules.[44,45] All of these QM calculations were done using the Gaussian'09 (G'09) package.[67] The G'09 "VeryTight" geometry optimization and "UltraFine" DFT numerical integration settings were applied. D_{2h} symmetry restrictions were imposed when composing the Z-matrix for G'09 to obtain the optimized equilibrium molecular geometry. However, the accounting of symmetry for the geometry optimization with G'09 and the evaluation of harmonic force constants was turned off because different symmetries of displaced configurations lead to poor results for the quartic force constants after the numerical differentiation.[43] Additional molecular properties, required for the perturbation theory calculations, such as cubic and quartic force constants and higher derivatives of dipole moment and polarizability components, were evaluated using numerical differentiation of basic G'09 molecular properties in normal coordinates.

The harmonic frequencies, representation of vibrational modes in internal coordinates, as well as Cartesian coordinate displacements along normal coordinates were calculated using the standard Wilson method. All anharmonic vibrational computations, except the electronic structure ones, were performed with the aid of our software package ANCO (acronym for Analysis of Normal Coordinates),[43] written in Fortran and designed for anharmonic vibrational normal coordinate calculations. The ANCO package is available for Windows and Linux operating systems.

The molecular model and the numbering of atoms of the porphin are presented in Figure 1 (reproduced in full size in the Supporting Information as Figure S1). The molecular geometry defined in terms of a G'09 Z-matrix and Cartesian coordinates in the standard orientation of Cartesian axes is presented in Supporting Information Table S1. Table 1 presents the values of optimized geometrical parameters (bond lengths and valence angles) in comparison with literature data. We did not include the experimental X-ray results for porphin because they show a lower symmetry of porphin.[3]

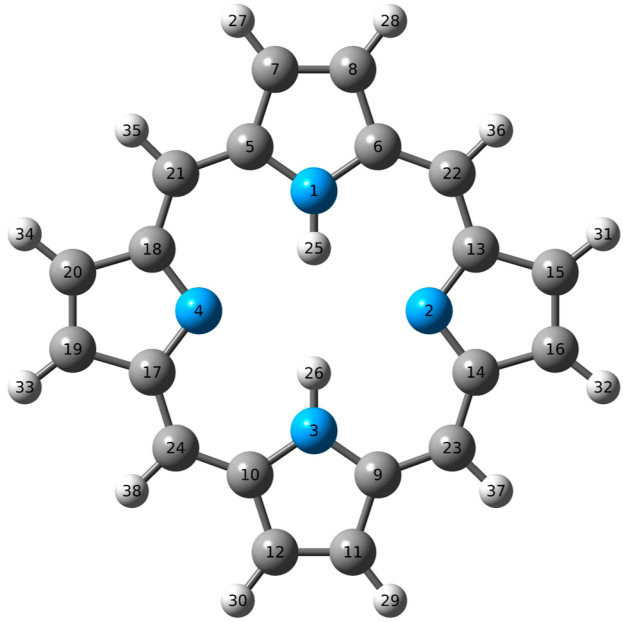

Figure 1. Free-base porphin molecular model and numbering of atoms.

Evaluation of normal modes in the space of internal vibrational coordinates requires an initial choice of valence coordinates. In principle, any full and independent set of valence internal coordinates can be used for a QM force field originally expressed in Cartesian coordinates. However, some sets of internal coordinates are preferable as they are closer to the normal modes. Therefore, the transformation matrix connecting internal and normal coordinates becomes quasi-diagonal, which makes it easier to interpret the normal modes in terms of valence (local symmetry) internal coordinates. This procedure is usually part of "a vibrational assignment", which should not be confused with the assignment of observed bands to fundamental $0 \rightarrow 1$ transitions. It is important to remember that the usefulness of the vibrational assignment in the former sense can be limited in some cases, especially for large molecules. First, normal modes can be complex linear combinations without any dominant part of properly chosen internal coordinates. In this case, available visualization software for normal vibrations can be utilized to help describe the vibrational forms in terms of standard terminology (such as twisting, wagging, scissoring, etc.). Second, fundamental transitions can be strongly mixed with other states due to Fermi and some types of D−D resonances. In this situation, even the assignment of observed bands to certain theoretical fundamental transitions can have an element of arbitrariness. For these reasons, we did not attempt to make a new careful analysis of the assignments of the vibrational mode, and we refer a reader to existing publications on normal coordinate analyses for porphin.[17−29]

However, the molecule of porphin is an interesting example of a polycyclic molecule, for which it is very difficult to introduce a full and nonredundant set of local symmetry coordinates.[68] For this reason, we composed such a set of coordinates using a combined technique. Namely, for the four pyrrole rings, we used the elegant set of independent local symmetry coordinates suggested in ref 69. The remaining redundancies in the 16-membered internal ring of heavy atoms were eliminated using an automated technique proposed in ref

dx.doi.org/10.1021/jp5077092 | J. Phys. Chem. A 2015, 119, 1616−1627

Table 1. Theoretical DFT-B3LYP/6-31+G(d,p) Quantum Mechanical Geometrical Parameters (Ångstroms, Degrees) of the Porphin Molecule in Comparison with Literature Data[a]

geometrical parameter	simplified designation	this work, 6-31+G(d,p)	this work,[b] cc-pVTZ	ref 27, 6-31G(d,p)	ref 31, 6-31G(d)
N(2)−C(13)	N−α	1.3642	1.3582	1.3638	1.364
C(13)−C(15)	α−β	1.4609	1.4561	1.4592	1.460
C(13)−C(22)	α−m	1.4013	1.3952	1.4004	1.400
C(15)−H(31)	β−H	1.0828	1.0784	1.0826	1.083
C(16)−C(15)	β−β	1.3590	1.3509	1.3568	1.356
C(22)−H(36)	m−H	1.0859	1.0817	1.0857	1.086
N(1)−C(5)	N−α'	1.3732	1.3677	1.3721	1.372
C(5)−C(7)	α'−β'	1.4359	1.4304	1.4353	1.435
C(5)−C(21)	α'−m	1.3954	1.3889	1.3932	1.394
C(7)−H(27)	β'−H	1.0815	1.0772	1.0813	1.082
C(8)−C(7)	β'−β'	1.3741	1.3670	1.3714	1.372
N(1)−H(25)	N−H	1.0148	1.0105	1.0145	1.015
∠C(5)−N(1)−H(25)	H−N−α'	124.57	124.55		124.6
∠C(5)−N(1)−C(6)	α'−N−α'	110.86	110.91		110.9
∠N(1)−C(5)−C(7)	N−α'−β'	106.57	106.51		106.5
∠C(5)−C(7)−H(27)	α'−β'−H	124.39	124.37		124.3
∠C(5)−C(7)−C(8)	α'−β'−β'	108.00	108.04		108.0
∠N(1)−C(5)−C(21)	N−α'−m	125.60	125.63		125.5
∠C(5)−C(21)−H(35)	α'−m−H	115.85	115.92		115.9
∠C(13)−N(2)−C(14)	α−N−α	105.62	105.81		105.4
∠N(2)−C(13)−C(15)	N−α−β	111.01	110.83		111.1
∠C(17)−C(19)−H(33)	α−β−H	125.45	125.43		125.4
∠C(13)−C(15)−C(16)	α−β−β	106.18	106.27		106.2
∠N(2)−C(13)−C(22)	N−α−m	125.44	125.59		125.5
∠C(13)−C(22)−H(36)	α−m−H	116.95	116.94		
∠C(5)−C(21)−C(18)	α−m−α'	127.20	127.14		127.1

[a]The abbreviation for the basis set 6-31G**, used in ref 27 is an equivalent of 6-31G(d,p), and the abbreviation 6-31G*, used in ref 31 is an equivalent of 6-31G(d). [b]The calculation for the basis set cc-pVTZ was also done in ref 75, but the results were published for bond lengths only.

70. This method is based on a reduction of the zero-eigenvalue subset of the full coordinate system G-matrix eigenvector matrix C to a special form with a unity-matrix sub-block, the dimension of which is equal to the number of redundant coordinates M_R (and zero eigenvalues, of course). This reduction is conducted in $j = 1...M_R$ steps and is based on a choice of the leading element in the $(M+j)$th column of the C-matrix, optional permutation of rows, and adding other columns from the $M + 1$ to $M + M_R$ subset to cancel unwanted nonzero elements. Once this process is accomplished, the rows of the unity-matrix sub-block correspond to redundant coordinates.[70] These internal coordinates can be simply omitted, and the remaining set of coordinates represents a full nonredundant set of internal (local symmetry) coordinates. Such a set, along with the Cartesian coordinates for porphin, is presented in the Supporting Information Tables S2−S4. It should be noted that the requirement of using an internal coordinate representation for the harmonic force field is vital in the case of the SQM technique that needs a correspondence between scale factors and adjustable blocks of the force constant matrix. When using the VPT2 approach, the normal coordinates can be defined directly in Cartesian coordinates. This obviates the need for a complex procedure of building nonredundant sets of internal (local symmetry) coordinates.

3.2. Porphin Quartic Force Field, Dipole Moment, and Polarizability Component Cubic Surfaces. The interaction of the employed software package ANCO with the G'09 package is arranged through automated generation, processing, and reading of input/output files in text format. For example, ANCO generates an input file for G'09 with Cartesian coordinates of molecular configurations shifted along normal coordinates and some keywords requesting computation of the Cartesian harmonic force constants matrix (Hessian) without geometry optimization. Afterward, when the electronic problem is solved, the G'09 output checkpoint files are converted into text format and processed by ANCO, which extracts the Hessian and other desired molecular properties.

The semi-diagonal (up to three different modes) quartic PESs were obtained by the one- and two-dimensional numerical differentiation of Hessians in normal coordinates, using the five point equidistant grids and a 0.02 Å × (amu)$^{1/2}$ step size

$$\phi_{ijk} = \frac{8(\phi_{jk}(+\delta q_i) - \phi_{jk}(-\delta q_i)) - (\phi_{jk}(+2\delta q_i) - \phi_{jk}(-2\delta q_i))}{12\delta q_i} \quad (3.1)$$

$$\phi_{iijk} = \frac{16(\phi_{jk}(+\delta q_i) + \phi_{jk}(-\delta q_i)) - (\phi_{jk}(+2\delta q_i) + \phi_{jk}(-2\delta q_i)) - 30\phi_{jk}(0)}{12\delta q_i^2} \quad (3.2)$$

Calculation of the cubic surfaces of the dipole moment components was performed by the single and double differentiation of the analytic dipole moments, while the polarizability (α) second derivatives were calculated by double differentiation of polarizability tensor components. The third derivatives of α were assumed nil.

3.3. Treatment of Resonances and the Variational Stage (VPT2+*WK*). In this work, we have employed the method of detecting resonances, compatible with the operator version of CVPT.[43,71] In the framework of this approach, any Hamiltonian term is considered resonant if a numerical coefficient of a corresponding S operator exceeds a certain dimensionless cutoff parameter (typically 0.05−0.50) and the corresponding "resonance denominator" is less than another threshold value expressed in cm^{-1} (typically 200−600 cm^{-1}).[43,71] It is not difficult to figure out what is the equivalent criterion for the customary VPT2+*WK* treatment. Namely, for FRs of kinds $2\omega_r \approx \omega_s$ (type I) and $\omega_r + \omega_s \approx \omega_t$ (type II), respectively, the following quantities should not exceed the chosen threshold cutoff parameter $\Xi^* = 0.08$ to be considered as nonresonant

$$\Xi^{(I)} = \frac{\sqrt{2}}{8}\left|\frac{\phi_{rrs}}{2\omega_r - \omega_s}\right| < \Xi^* \quad (3.3)$$

$$\Xi^{(II)} = \frac{\sqrt{2}}{4}\left|\frac{\phi_{rst}}{\omega_r + \omega_s - \omega_t}\right| < \Xi^* \quad (3.4)$$

At the same time, the maximum allowed values of denominators in eqs 3.3 and 3.4 for resonant terms should not exceed the chosen value of 300 cm^{-1}. Our choice of resonance parameters produced 21 type I and 369 type II FRs.

For the D−D resonances, we imposed the following restrictions. First, the second-order resonance denominators should be less than 250 cm^{-1}, and, second, the values of D−D resonance constants K should be greater than 10 cm^{-1}. Further discussion about the synchronization of the resonance choices for VPT2 and CVPT2 methods and physically meaningful resonance criteria can be found in ref 71.

Finally, it should be noted that during the variational stage of the VPT2+*WK* calculation, we employed the harmonic oscillator basis set restricted to 2 quanta of total vibrational excitation, a choice that produced 5994 functions of 8 symmetry types. The maximum size of the symmetry block was 894 functions for the A_g species. Each block of the Hamiltonian matrix was diagonalized separately. This example demonstrates the convenience of the VPT2+*WK* method in comparison to the full variational method that would require a bigger basis set than here even for a four-atomic molecule.

4. RESULTS AND DISCUSSION

In this section, we summarize the most interesting features of the interpretation of the spectrum, ordered by symmetry blocks. Because we need to establish a correspondence between observed band centers and anharmonic states, omitting the transitions with nil values of allowed intensities greatly reduces the number of states of interest. The analysis of assignments of observed fundamental bands and interesting features are presented below in detail. Porphin spectra were studied experimentally by many methods; IR spectra were reported in the solid state and in matrix-isolated form in refs 4−8; RR spectra in refs 9−11; nonresonance Raman spectra in ref 12; luminescence and fluorescence spectra in refs 13−15; and finally INS spectra in ref 16. A summary of observed spectra is presented in Tables 4 and S1 of ref 16.

4.1. Symmetry Block A_g (19 In-Plane Species ν_1−ν_{19}, Raman-Active), Table 2. An excellent literature discussion of the observations and assignments of these symmetry species can be found in ref 12. Essential experimental data of observed spectra can also be found in ref 14. The highest ν_1 frequency, the N−H vibration, has low intensity and was not observed. In the C−H frequency region, only ν_2 has been observed experimentally in the INS spectrum.[16] The predicted fundamental ν_3 lies close and may overlap. Both fundamentals are strongly affected by FRs. The ν_3 mode resonates with $2 \times \nu_6$, $2 \times \nu_{69}$, and, to a smaller extent, $\nu_6 + \nu_7$ [DP values of 3119.9, 3120.8, 3093.4, and 3064.9 cm^{-1}, accordingly], and as a result, ν_3 is shifted up to the new value of 3134.6 cm^{-1} by 14.7 cm^{-1}. The ν_4 mode (DP value of 3058.4 cm^{-1}) resonates with four overtones [FR(rr,s) type I] and seven binary combination bands [FR(rs,t) type II]; the final ν_4 frequency after diagonalization is 3070.9 cm^{-1}, shifted by 12.5 cm^{-1}.

Table 2. Calculated and Observed Fundamental Frequencies (in cm^{-1}) of Porphin of A_g Symmetry (In-Plane; Raman-Active)[a]

mode	harmonic	anharm., deperturb.	anharm., perturbed	intensity[b]	observed	error
ν_1	3599.6	3392.9	3392.9	0.44		
ν_2	3264.4	3137.5	3137.3	112.52	3146[c]	−8.5
ν_3	3249.7	3119.9	3134.6	120.47		
ν_4	3195.4	3058.4	3071.0	59.69		
ν_5	1648.0	1611.8	1614.5	75.29	1614	0.5
ν_6	1593.9	1561.6	1563.2	147.29	1575	−11.8
ν_7	1540.0	1507.5	1506.1	134.78	1502	4.1
ν_8	1466.8	1437.9	1437.0	53.33	1424	13.0
ν_9	1434.4	1401.8	1403.9	105.29	1400	3.9
ν_{10}	1385.4	1356.8	1358.0	19.28	1360	−2.0
ν_{11}	1205.9	1182.5	1182.1	18.00	1182, 1177	0.1
ν_{12}	1089.7	1074.0	1074.4	7.49	1064	10.4
ν_{13}	1082.7	1066.0	1065.6	4.19	1061	5.0
ν_{14}	1009.8	993.7	994.0	32.96	988	5.7
ν_{15}	972.5	958.4	958.4	60.97	952	6.4
ν_{16}	736.9	727.3	727.4	14.83	736[d]	−8.6
ν_{17}	731.1	722.1	722.1	17.05	722, 723	0.1
ν_{18}	309.0	304.8	304.9	224.29	305	−0.1
ν_{19}	155.0	149.0	149.1	228.81	155	−5.9

[a]The observed values are taken from refs 12 and 15, with exceptions (see additional footnotes). [b]Intensities are calculated as absolute normalized differential cross sections, 10^{-48} cm^6/sr. [c]Reference 16. [d]Reference 9.

dx.doi.org/10.1021/jp5077092 | J. Phys. Chem. A 2015, 119, 1616−1627

Our calculation answers the essential question posed by Kozlowski et al. in ref 12 concerning the assignment of observed bands at 1400 and 1384 cm^{-1}. The predicted values ν_9 = 1403.9 cm^{-1} and $\nu_{33}(B_{1g})$ = 1385.7 cm^{-1} suggest a reversal of the former assignment, as was anticipated but not confirmed in ref 12.

The fundamentals ν_5, ν_6, ν_7, ν_9, and ν_{10} of A_g symmetry are weakly (<3 cm^{-1}) shifted due to FRs even after strong mixing with other states. Fundamentals ν_1–ν_2 and ν_{11}–ν_{19} are free of strong FRs and produce nearly pure anharmonic states. The overall agreement between predicted and observed bands in this symmetry block is very good; the maximum discrepancy does not exceed 12 cm^{-1} and in four cases is less than 1 cm^{-1}.

4.2. Symmetry Block A_u (Eight Out-of-Plane Species ν_{20}–ν_{27}, IR- and Raman-Inactive), Table 3. Fundamental transitions of this symmetry type were observed only in the INS spectra.[16] All fundamentals are practically free of FRs. The data on the symmetry of observed bands in ref 16 are a little contradictory; the A_u bands at 895 and 691 cm^{-1} in Table 4 in ref 16 are indicated in the paper's Supporting Information Table S1[16] as belonging to different symmetry species (B_{3g} and B_{1u}, accordingly). The calculated values of ν_{20} and ν_{21} are close to each other, 896.2 and 897.1 cm^{-1}; they can be attributed to the observed bands at 908 and 895 cm^{-1}. Another pair of predicted close-lying fundamentals, ν_{23} (684.4 cm^{-1}) and ν_{24} (669.7 cm^{-1}), seems to correspond to the observed band at 684 cm^{-1} rather than that at 691 cm^{-1}, as indicated in Table 4 of ref 16. The predicted fundamental ν_{25} (472.9 cm^{-1}) is in good agreement with an observed band at 480 cm^{-1}. Two predicted low frequencies, ν_{26} (283.3 cm^{-1}) and ν_{27} (35.9 cm^{-1}), are not a good match with observed values (see Table 3). This discrepancy can be expected from a well-known deficiency of VPT2; it cannot provide a good modeling of low frequencies due to the specific form of the potential well. In such cases, a harmonic frequency can be a good estimation of the expected value.

Table 3. Calculated and Observed Fundamental Frequencies (in cm^{-1}) of Porphin of A_u Symmetry (Out-of-Plane; IR- and Raman-Inactive)[a]

mode	harmonic	anharm., deperturb.	anharm., perturbed	intensity	observed	error
ν_{20}	921.5	895.9	896.2	0.0	895, 908	11.8
ν_{21}	912.8	896.9	897.1	0.0	882	−15.1
ν_{22}	858.7	837.7	837.4	0.0	831	−6.4
ν_{23}	703.0	684.6	684.4	0.0	684	−0.4
ν_{24}	687.0	669.9	669.7	0.0		
ν_{25}	485.9	472.9	472.9	0.0	480	7.1
ν_{26}	300.0	283.3	283.3	0.0	303	19.7
ν_{27}	69.2	35.9	35.9	0.0	70, 72	34.1

[a]The observed values are taken from ref 16.

4.3. Symmetry Block B_{1g} (18 In-Plane Species ν_{28}–ν_{45}, Raman-Active), Table 4. This symmetry block shows generally good agreement (see Table 4) between the predicted fundamentals and observed values, obtained in RR[9−11] and fluorescence spectra (MLS).[14,15] Although mixing of the zero-order states is big for some fundamentals (ν_{30}–ν_{34}, ν_{37}), resonance shifts do not exceed 5 cm^{-1}. Fundamentals from this block only participate in FRs of the type (*rs*,*t*) and not (*rr*,*s*) due to the symmetry restriction. The fundamental ν_{33} participates in a complex polyad with double combination states and is delocalized between about seven anharmonic states. As stated above (section 4.1), we reassigned the observed band at 1384 cm^{-1} to ν_{33}, and not 1400 cm^{-1} as suggested in ref 12. Finally, the observed band at 3109 cm^{-1} should be attributed to both to ν_{28} and ν_{29} on the grounds of calculated values.

Table 4. Calculated and Observed Fundamental Frequencies (in cm^{-1}) of Porphin of B_{1g} Symmetry (In-plane; Raman-Active)

mode	harmonic	anharm., deperturb.	anharm., perturbed	intensity[a]	observed	error
ν_{28}	3247.3	3121.0	3120.6	43.88	3109[b]	−11.6
ν_{29}	3228.9	3103.1	3103.0	48.72		
ν_{30}	3195.3	3058.4	3054.6	42.48		
ν_{31}	1632.2	1594.9	1600.1	0.01	1599,[c] 1600[d]	−0.1
ν_{32}	1532.4	1496.8	1495.1	10.68	1497[b]	−1.9
ν_{33}	1414.3	1380.3	1385.7	18.89	1388,[b] 1384[e]	1.7
ν_{34}	1389.1	1361.6	1362.9	11.32	1352,[b] 1350[e]	10.9
ν_{35}	1351.4	1321.3	1323.4	38.03	1316,[b] 1314[c]	7.4
ν_{36}	1261.4	1232.4	1230.8	2.52	1221,[b] 1224[c]	9.8
ν_{37}	1217.6	1195.6	1194.0	0.48	1192,[d] 1177[b]	2.0
ν_{38}	1166.2	1145.5	1144.8	0.00	1138,[d] 1134[b]	10.8
ν_{39}	1026.9	1009.6	1010.7	4.49	1004,[d] 1001[b]	6.7
ν_{40}	997.3	980.1	980.6	1.97	988,[d] 972[b]	−7.4
ν_{41}	817.4	807.8	808.4	1.46	805[d]	3.4
ν_{42}	796.4	788.3	788.3	0.00	786[b,d]	2.3
ν_{43}	419.2	411.4	411.8	0.53	418[d]	−6.2
ν_{44}	395.7	389.7	389.7	0.08	389[d]	0.7
ν_{45}	101.4	86.4	86.4	325.03	109[d]	−22.6

[a]Intensities are calculated as absolute normalized differential cross sections, 10^{-48} cm^6/sr. [b]Observed values taken from ref 15. [c]Observed values taken from ref 9. [d]Observed values taken from ref 11. [e]Observed values taken from ref 12.

4.4. Symmetry Block B_{1u} (10 Out-of-Plane Species ν_{46}–ν_{55}, IR-Active), Table 5. The most reliable experimental data on transitions of B_{1u}, B_{2u}, and B_{3u} symmetry types

Table 5. Calculated and Observed Fundamental Frequencies (in cm^{-1}) of Porphin of B_{1u} Symmetry (Out-of-Plane; IR-Active)[a]

mode	harmonic	anharm., deperturb.	anharm., perturbed	intensity, km/mol	observed	error
ν_{46}	876.2	852.0	852.5	163.49	852	0.5
ν_{47}	800.1	780.2	780.1	54.41	785	−4.9
ν_{48}	792.0	764.6	768.5	99.70	773	−4.5
ν_{49}	745.7	712.1	710.3	2.59	731	−20.7
ν_{50}	708.5	693.5	691.2	47.51	691	0.2
ν_{51}	653.6	636.4	636.0	0.12	639	−3.0
ν_{52}	335.3	322.1	322.1	5.72	335	−12.9
ν_{53}	212.2	194.4	194.7	1.75	219	−24.3
ν_{54}	95.8	66.1	66.1	7.29	94[b]	−27.9
ν_{55}	54.9	33.3	33.0	0.00		

[a]The observed values are taken from ref 8, with one exception (see footnote *b*). [b]Reference 16.

dx.doi.org/10.1021/jp5077092 | J. Phys. Chem. A 2015, 119, 1616−1627

observed in the IR are available in refs 7 and 8. A detailed discussion and comparison with calculated (SQM) vibrations of porphin can be found in ref 21. In this symmetry block, the highest calculated frequency of ν_{46} is 852.5 cm^{-1} because all vibrations are out-of-plane. The calculation shows that among B_{1u} fundamentals, there is only one strong FR coupling between ν_{48} and combination state $\nu_{62} + \nu_{107}$ that produces a doublet of 768.5 and 769.9 cm^{-1}. Indeed, there are two observed closely lying bands, 773 and 774 cm^{-1}.[7,8] Our calculation supports the conclusion drawn in ref 21. about the assignment of the band at 335 cm^{-1} to ν_{48} and not to the B_{2u} transition as was originally interpreted in the experimental studies.[7,8]

The overall agreement between calculated and observed frequencies for ν_{46}, ν_{47}, ν_{48}, ν_{50}, and ν_{51} is very good (error < 5 cm^{-1}). The only exceptions are ν_{49} and frequencies below 400 cm^{-1}, the anharmonic character of which is modeled with less accuracy by VPT2. Comparison of our calculated and observed[8] intensities shows reasonable semiquantitative agreement.

4.5. Symmetry Block B_{2g} (Nine Out-of-Plane Species ν_{56}–ν_{64}, Raman-Active), Table 6. The out-of-plane B_{2g} and

Table 6. Calculated and Observed Fundamental Frequencies (in cm^{-1}) of Porphin of B_{2g} Symmetry (Out-of-Plane; Raman-Active)[a]

mode	harmonic	anharm., deperturb.	anharm., perturbed	intensity[b]	observed	error
ν_{56}	916.7	900.2	900.4	1.36	882	18.4
ν_{57}	868.0	842.0	844.3	1.94	843	1.3
ν_{58}	789.3	773.1	772.3	0.10	771	1.3
ν_{59}	708.0	661.3	682.6	0.06	691	−8.4
ν_{60}	694.0	668.0	644.8	0.40	628	16.8
ν_{61}	653.0	631.7	631.5	1.04	628	3.5
ν_{62}	430.9	419.5	419.6	0.17	415, 426	4.6
ν_{63}	189.5	171.2	171.2	14.71	166, 200	5.2
ν_{64}	132.0	112.4	112.4	3.29		

[a]The observed values are taken from ref 16. [b]Intensities are calculated as absolute normalized differential cross sections, 10^{-48} cm^6/sr.

B_{3g} species derive their Raman intensity entirely from vibronic coupling, and such transitions must carry little intensity.[12] The calculation confirms this conclusion; only low-frequencies ν_{63} (B_{2g}) and ν_{89} (B_{3g}) have appreciable predicted intensity. The main source of experimental data is the INS spectra obtained in ref 16.

Two B_{2g} fundamentals, ν_{59} and ν_{60}, manifest an interesting and rare effect, 1−1 D−D resonance. The coupling matrix element between zero-order states is −17.9 cm^{-1}, which increases the difference between these two closely lying (6.7 cm^{-1}) DP levels to 37.7 cm^{-1}. The final values after diagonalization are 682.5 and 644.8 cm^{-1}, which reasonably agree with the observed pair of 691 and 628 cm^{-1}. It is most likely that the band at 628 cm^{-1} also belongs to ν_{61}. This fundamental is in heavy FR with combination states $\nu_{52} + \nu_{108}$ and $\nu_{26} + \nu_{81}$, producing a triplet of 629.8, 631.5, and 635.1 cm^{-1}. The remaining B_{2g} fundamentals are free from FRs.

4.6. Symmetry Block B_{2u} (18 In-Plane Species ν_{65}–ν_{82}, IR-active), Table 7. Reliable experimental data on transitions of this symmetry type in the IR can be found refs 7 and 8, and a detailed discussion and comparison with calculated (SQM) vibrations of porphin is presented in ref 21. Of all fundamentals of B_{2u} symmetry, 10 states are heavily involved in resonance

Table 7. Calculated and Observed Fundamental Frequencies (in cm^{-1}) of Porphin of B_{2u} Symmetry (Out-of-Plane; IR-Active)[a]

mode	harmonic	anharm., deperturb.	anharm., perturbed	intensity, km/mol	observed	error
ν_{65}	3249.6	3119.7	3132.4	31.03	3124	8.4
ν_{66}	3247.3	3121.3	3119.8	1.43	3118, 3112	
ν_{67}	3195.2	3058.1	3062.3	8.39	3045	17.3
ν_{68}	1636.4	1601.0	1599.7	21.10	1609	−0.3
ν_{69}	1582.3	1547.9	1547.9	37.13	1540	7.9
ν_{70}	1529.2	1496.3	1492.6	4.41	1490	2.6
ν_{71}	1443.3	1410.4	1409.7	13.92	1406	3.7
ν_{72}	1386.6	1355.5	1357.6	2.86	1357	0.6
ν_{73}	1279.2	1253.2	1252.4	0.03	1255	−2.6
ν_{74}	1263.6	1235.5	1232.6	56.57	1228	4.6
ν_{75}	1184.1	1161.8	1162.6	0.01	1156	6.6
ν_{76}	1079.9	1063.4	1063.4	44.44	1054	9.4
ν_{77}	1008.4	991.5	992.5	8.16	986	6.5
ν_{78}	969.7	956.4	956.4	85.91	951	5.4
ν_{79}	790.9	783.5	783.7	0.18		
ν_{80}	756.5	747.3	744.1	29.65	745	−0.9
ν_{81}	357.4	351.3	351.4	11.19	353[b]	−1.6
ν_{82}	291.5	285.4	285.4	0.18	282, 284[c]	

[a]The observed values are taken from ref 8, with two exceptions (see the additional footnotes). [b]Reference 6. [c]Reference 16.

couplings. However, a significant resonance shift (12.7 cm^{-1}) is observed only for the pair of ν_{65} and the combination state $\nu_6 + \nu_{69}$. The corresponding cubic force constant $\phi_{6,65,69}$ = 45.9 cm^{-1} and the "resonance denominator" $(\omega_{65} - \omega_6 - \omega_{69})^{-1}$ is equal to 73.4 cm^{-1}, which corresponds to a rather strong value of the resonance index Ω_{FR} = 0.22.[43,72] After the diagonalization of the effective Hamiltonian, the DP values of ν_{65} and $\nu_6 + \nu_{69}$ (3119.7 and 3105.2 cm^{-1}) are moved apart to the final values of 3132.4 and 3097.2 cm^{-1}, and the originally very weak band $\nu_6 + \nu_{69}$ gains about a quarter of the intensity of ν_{65}. There are two observed bands of nearly equal intensity in this region, 3124 and 3112 cm^{-1}.[8] The literature assignment of the latter is ν_{66}, but its calculated intensity is an order of magnitude smaller than that for ν_{65}. The same result about the intensity ratio for ν_{65} and ν_{66} was obtained in ref 21. Therefore, we believe that a weak band ν_{66} can either be hiding under a stronger resonance B_{2u} band at 3112 cm^{-1} for $\nu_6 + \nu_{69}$ or correspond to a B_{3u} band at 3118 cm^{-1}. Indeed, the calculation of B_{3u} species predicts only three strong bands (3056.5, 3103.7, and 3140.0 cm^{-1}) in this region, while here there are four observed bands (3042, 3088, 3118, and 3128 cm^{-1}), all assigned to B_{3u}.[8]

The correspondence between calculated and observed values for the majority of fundamentals of B_{2u} symmetry type is very good; the errors typically do not exceed 10 cm^{-1}; see Table 7. There is another remarkable observation. As we said above, although 10 fundamentals participate heavily in FRs, for 9 of them, the calculated resonance shift is smaller than 4 cm^{-1}. This is an interesting theoretical phenomenon; for a big molecule with large density of states, like in porphin, the resonance shifts are typically small. It can be explained by the multitude of closely lying dark states, each of which is weakly interacting with the main bright state and in aggregate-limiting perturbation frequency shifts.

4.7. Symmetry Block B_{3g} (Eight Out-of-Plane Species ν_{83}–ν_{90}, Raman-Active), Table 8. This symmetry block, like

dx.doi.org/10.1021/jp5077092 | J. Phys. Chem. A 2015, 119, 1616−1627

Table 8. Calculated and Observed Fundamental Frequencies (in cm^{-1}) of Porphin of B_{3g} Symmetry (Out-of-Plane; Raman-Active)[a]

mode	harmonic	anharm., deperturb.	anharm., perturbed	intensity[b]	observed	error
ν_{83}	919.4	896.3	896.3	0.76	895	1.3
ν_{84}	866.0	843.8	844.3	2.03	843	1.3
ν_{85}	786.7	769.8	769.0	0.01	771	−2.0
ν_{86}	711.1	694.4	694.9	1.07	691	3.9
ν_{87}	675.6	646.7	646.3	0.89	647	−0.7
ν_{88}	445.0	426.5	426.7	0.13	426, 436	0.7
ν_{89}	208.8	188.3	188.2	14.18	200, 204	−11.8
ν_{90}	133.5	112.4	112.4	0.50	145	−32.6

[a]The observed values are taken from ref 16. [b]Intensities are calculated as absolute normalized differential cross sections, 10^{-48} cm^6/sr.

B_{2g}, carries only eight low-frequency fundamentals with very low Raman intensity, so that INS spectra[16] are the only source of experimental information.

The fundamental state ν_{66} is involved in FR with combination states $\nu_{45} + \nu_{59}$ and $\nu_{45} + \nu_{60}$, but resulting energy levels are separated by only 1.4 cm^{-1}. The remaining fundamentals are free from FRs. The agreement between observed and calculated frequencies of fundamentals is very good (error < 4 cm^{-1}) from 450 cm^{-1} and higher. For very low frequencies (observed value of ν_{66} = 145 cm^{-1}), the error reaches 33 cm^{-1}. This deficiency of VPT2 does not spoil the whole picture because low frequencies are difficult to measure and their studies are often done separately.

4.8. Symmetry Block B_{3u} (18 In-Plane Species ν_{91}–ν_{108}, IR-Active), Table 9. Among the fundamentals of B_{3u} symmetry, 13 states (ν_{91-93}, ν_{97}, ν_{99-103}, $\nu_{105-108}$) are weakly coupled by resonances. Except for the N–H frequency ν_{91}, the deviations between calculated and observed bands do not exceed 17 cm^{-1}. At the same time, the deviations are typically positive, showing a systematic QM deficiency. For example, for three C–H vibrations, the errors are in the range of 12.0–15.7 cm^{-1}.

Table 9. Calculated and Observed Fundamental Frequencies (in cm^{-1}) of Porphin of B_{3u} Symmetry (In-Plane; IR-Active)[a]

mode	harmonic	anharm., deperturb.	anharm., perturbed	intensity, km/mol	observed	error
ν_{91}	3556.8	3355.8	3355.8	70.87	3324	31.8
ν_{92}	3264.3	3136.4	3140.0	9.31	3128	12.0
ν_{93}	3229.0	3101.9	3103.7	5.86	3088	15.7
ν_{94}	3195.3	3058.1	3056.5	10.33	3042	14.5
ν_{95}	1562.0	1529.9	1531.4	11.38	1522	9.4
ν_{96}	1549.1	1510.8	1506.4	0.04	1507	−0.6
ν_{97}	1440.9	1410.4	1410.3	10.32	1412	−1.7
ν_{98}	1436.2	1405.0	1400.5	23.61	1396	4.5
ν_{99}	1316.8	1291.6	1290.4	1.81	1287	3.4
ν_{100}	1232.3	1213.3	1213.5	0.72		
ν_{101}	1170.2	1148.6	1147.1	24.65	1134	13.1
ν_{102}	1075.4	1059.8	1059.7	48.29	1043	−16.7
ν_{103}	1021.6	1004.8	1005.2	0.02	994	11.2
ν_{104}	991.5	976.6	975.6	50.15	971	4.6
ν_{105}	795.1	787.4	788.5	1.75	780	8.5
ν_{106}	738.4	730.7	730.4	30.46	723	7.4
ν_{107}	357.0	350.1	350.1	8.76	357	−6.9
ν_{108}	316.1	308.5	308.5	2.37	310	−1.5

[a]The observed values are taken from ref 8.

In our opinion, the literature assignment of ν_{100} to the observed[8] band at 1177 cm^{-1} with a relative intensity of 7.6 10^{-48} cm^6/sr is incorrect as the calculated value is 1213.5 cm^{-1} with low intensity. The band at 1177 cm^{-1} is probably not a fundamental, but the prediction cannot securely describe its assignment.

The fundamental ν_{95} is highly delocalized in a polyad of about eight states in the calculated range of 1513.5–1537.6 cm^{-1}. The observed band of 1522 cm^{-1} agrees well with the calculation. In this symmetry block, we again see the same picture of multiple resonances and small aggregate shifts (<5.0 cm^{-1}) of fundamental levels. It looks like there is a general regularity that with the increase of the size of the molecule, the increasing density of levels limits the effect of resonance shifts. For example, in formaldehyde with six modes, two of them (ν_1, ν_5) have resonance shifts on the order of 30 cm^{-1}. In porphin with 108 modes, only 5 fundamentals (ν_3, ν_4, ν_{59}, ν_{60}, ν_{65}) have resonance shifts of more than 10 cm^{-1}, typically <15 cm^{-1}.

5. CONCLUSIONS

The primary goal of this work is a demonstration of the power of recent advances in the theory of anharmonic vibrations of large molecules. This power is three-fold, (1) a maximum automation of the calculations, (2) no dependence on empirical information and adjustments, and (3) extensive calculated results, sufficient for a confident analysis of experimental spectra.

For the first time, in this work, we have calculated fully ab initio anharmonic vibrational frequencies and intensities of a biologically important 38-atom porphin molecule. Although our approach is based on a relatively inexpensive QM model, the hybrid DFT functional B3LYP, and a medium-size basis set 6-31G+(d,p), the resulting values of fundamental frequencies are very close to the experimental counterparts, thereby obviating the need for empirical adjustments of the force field. The pleasing success of this modest QM model supports an earlier recognition of the cancellation of errors.[73,74]

We have shown that even for a large polycyclic molecule, it is possible to find a set of local symmetry coordinates using a semiautomated procedure that removes final redundancies after the introduction of local symmetry coordinates for standard fragments of smaller size.

The VPT2 method does not require the construction of independent sets of internal coordinates. Indeed, it is sufficient to define normal modes in Cartesian coordinates, as can be done entirely by starting from the QM Hessian expressed in Cartesian space. In addition, the VPT2 method does not require the manual choice of scale factors. It may seem surprising that a nonempirical anharmonic VPT2 calculation of fundamentals (and other transitions too) requires less manual work than SQM-based harmonic calculations.

We have observed an interesting theoretical phenomenon; for a large molecule with a high density of states, such as porphin, significant (>20 cm^{-1}) resonance shifts are less common than those in molecules of smaller size. This outcome is a consequence of multiple interactions with a high density of dark states. In addition, in many cases, fundamental states are heavily mixed with nearby states, causing broadening of observed bands.

dx.doi.org/10.1021/jp5077092 | J. Phys. Chem. A 2015, 119, 1616–1627

Success in predicting anharmonic spectra (IR and Raman) paves the way to subsequent studies of biomolecules by VPT2+*WK*.

■ ASSOCIATED CONTENT

Supporting Information

Two figures (S1 and S2) and four tables (S1−S4) with the geometry definition (G'09 Z-matrix) and the Cartesian, valence, and local symmetry coordinates of porphin are presented. This material is available free of charge via the Internet at http://pubs.acs.org.

■ AUTHOR INFORMATION

Corresponding Author

*E-mail: sergeyk@phys.chem.msu.ru. Tel.: 7 (495) 939-2950.

Notes

The authors declare no competing financial interest.

■ ACKNOWLEDGMENTS

The authors are deeply indebted to Prof. Norman C. Craig for the invaluable help reading the manuscript and editorial suggestions. A part of the VPT2 calculations were performed on the Chebyshev Supercomputer in Lomonosov Moscow State University.

■ REFERENCES

(1) Dolphin, D., Ed. *The Porphyrins*; Academic Press: New York, 1978/1979; Vols. *1*−*7*.
(2) Kadish, K. M., Smith, K. M., Guilard, R., Eds. *The Porphyrin Handbook*; Academic Press: New York, 1999; Vols. *1*−*10*.
(3) Chen, B. M. L.; Tulinsky, A. Redetermination of the Structure of Porphine. *J. Am. Chem. Soc.* **1972**, *94*, 4144−4151.
(4) Mason, S. F. The Infrared Spectra of N-Heteratomic Systems. Part I. The Porphins. *J. Chem. Soc.* **1958**, 976−982.
(5) Ogoshi, H.; Saito, Y.; Nakamoto, K. Infrared Spectra and Normal Coordinate Analysis of Metalloporphins. *J. Chem. Phys.* **1972**, *57*, 4194−4202.
(6) Gladkov, L. L.; Gradyushko, A. T.; Shulga, A. M.; Solovyov, K. N.; Starukhin, A. S. Experimental and Theoretical Investigation of Infrared Spectra of Porphin, Its Deuterated Derivatives and Their Metal Complexes. *J. Mol. Struct.* **1978**, *47*, 463−493.
(7) Radziszewski, J. G.; Waluk, J.; Michl, J. Site-Population Conserving and Site-Population Altering Photo-Orientation of Matrix-Isolated Free-Base Porphine by Double Proton Transfer: IR Dichroism and Vibrational Symmetry Assignments. *Chem. Phys.* **1989**, *136*, 165−180.
(8) Radziszewski, J. G.; Nepras, M. V.; Waluk, J.; Vogel, E.; Michl, J. Polarized Infrared Spectra of Photooriented Matrix-Isolated Free-Base Porphyrin Isotopomers. *J. Phys. Chem.* **1995**, *99*, 14254−14260.
(9) Verma, A. L.; Bernstein, H. J. Resonance Raman Spectra of Metal-Free Porphin and Some Porphyrins. *Biochem. Biophys. Res. Commun.* **1974**, *57*, 255−262.
(10) Plus, R.; Lutz, M. Study of Band IV of Porphin by Resonance Raman Spectroscopy. *Spectrosc. Lett.* **1974**, *7*, 73−84.
(11) Solovyov, K. N.; Gladkov, L. L.; Gradyushko, A. T.; Ksenofontova, N. M.; Shulga, A. M.; Starukhin, A. S. Resonance Raman Spectra of Deuterated Metalloporphins. *J. Mol. Struct.* **1978**, *45*, 267−305.
(12) Kozlowski, P. M.; Jarzecki, A. A.; Pulay, P.; Li, X.-Y.; Zgierski, M. Z. Vibrational Assignment and Definite Harmonic Force Field for Porphine. 2. Comparison with Nonresonance Raman Data. *J. Phys. Chem.* **1996**, *100*, 13985−13992.
(13) Kim, B. F.; Bohandy, J.; Jen, C. K. Optical Fluorescence Spectra of Porphins in Organic Crystalline Hosts. *Spectrochim. Acta, Part A* **1974**, *30*, 2031−2040.
(14) Radziszewski, J. G.; Waluk, J.; Michl, J. FT Visible Absorption Spectroscopy of Porphine in Noble Gas Matrices. *J. Mol. Spectrosc.* **1990**, *140*, 373−389.
(15) Radziszewski, J. G.; Waluk, J.; Nepras, M.; Michl, J. Fourier Transform Fluorescence and Phosphorescence of Porphine in Rare Gas Matrixes. *J. Phys. Chem.* **1991**, *95*, 1963−1969.
(16) Verdal, N.; Kozlowski, P. M.; Hudson, B. S. Inelastic Neutron Scattering Spectra of Free Base and Zinc Porphines: A Comparison with DFT-Based Vibrational Analysis. *J. Phys. Chem. A* **2005**, *109*, 5724−5733.
(17) Bohandy, J.; Kim, B. F. A Normal Mode Analysis of Free Base Porphin. *Spectrochim. Acta, Part A* **1980**, *36*, 463−466.
(18) Gladkov, L. L.; Solovyov, K. N. The Normal Coordinate Analysis of Porphin and Its Derivatives Based on the Solution of the Inverse Spectral Problem for Porphin and Cu Porphin — I. A Valence Force Field for In-Plane Vibrations of the Porphin Molecule. *Spectrochim. Acta, Part A* **1985**, *41*, 1437−1442.
(19) Li, X. Y.; Zgierski, M. Z. Porphine Force Field: In-Plane Normal Modes of Free-Base Porphine; Comparison with Metalloporphines and Structural Implications. *J. Phys. Chem.* **1991**, *95*, 4268−4287.
(20) Kozlowski, P. M.; Zgierski, M. Z.; Pulay, P. An Accurate In-Plane Force Field for Porphine. A Scaled Quantum Mechanical Study. *Chem. Phys. Lett.* **1995**, *247*, 379−385.
(21) Kozlowski, P. M.; Jarzecki, A. A.; Pulay, P. Vibrational Assignment and Definite Harmonic Force Field for Porphine. 1. Scaled Quantum Mechanical Results and Comparison with Empirical Force Field. *J. Phys. Chem.* **1996**, *100*, 7007−7013.
(22) Nguyen, K. A.; Day, P. N.; Pachter, R. Effects of Halogenation on the Ionized and Excited States of Free-Base and Zinc Porphyrins. *J. Chem. Phys.* **1999**, *110*, 9135−9144.
(23) Tazi, M.; Lagant, P.; Vergoten, G. Use of the Resonance Raman Intensities to Check the Density Functional Theory Derived Force Field of the Free Base Porphine. *J. Phys. Chem. A* **2000**, *104*, 618−625.
(24) Berezin, K. V.; Tatarenko, O. D.; Nechaev, V. V. Calculation of Out-of-Plane Vibrations of a Porphin Molecule. *J. Appl. Spectrosc.* **2002**, *69*, 534−539.
(25) Berezin, K. V.; Nechaev, V. V. A Force Field for Out-of-Plane Porphine Vibrations. *Rus. J. Phys. Chem. A* **2003**, *77*, 61−65.
(26) Berezin, K. V.; Tatarenko, O. D.; Nechaev, V. V. Force Field for the In-Plane Vibrations in Porphine. *Russ. J. Phys. Chem. A* **2003**, *77*, 115−120.
(27) Minaev, B.; Ågren, H. Theoretical DFT Study of Phosphorescence from Porphyrins. *Chem. Phys.* **2005**, *315*, 215−239.
(28) Minaev, B.; Wang, Y.-H.; Wang, C.-K.; Luo, Y.; Ågren, H. Density Functional Theory Study of Vibronic Structure of the First Absorption Q_x Band in Free-Base Porphin. *Spectrochim. Acta, Part A* **2006**, *65*, 308−323.
(29) Aydin, M. DFT and Raman Spectroscopy of Porphyrin Derivatives: Tetraphenylporphine (TPP). *Vib. Spectrosc.* **2013**, *68*, 141−152.
(30) Almlöf, J.; Fischer, T. H.; Gassman, P. G.; Ghosh, A.; Haeser, M. Electron Correlation in Tetrapyrroles: Ab Initio Calculations on Porphyrin and the Tautomers of Chlorin. *J. Phys. Chem.* **1993**, *97*, 10964−10970.
(31) Nguyen, K. A.; Day, P. N.; Pachter, R. Triplet Excited States of Free-Base Porphin and Its β-Octahalogenated Derivatives. *J. Phys. Chem. A* **2000**, *104*, 4748−4754.
(32) Pulay, P.; Fogarasi, G.; Pongor, G.; Boggs, J. E.; Vargha, A. Combination of Theoretical Ab Initio and Experimental Information to Obtain Reliable Harmonic Force Constants. Scaled Quantum Mechanical (QM) Force Fields for Glyoxal, Acrolein, Butadiene, Formaldehyde, and Ethylene. *J. Am. Chem. Soc.* **1983**, *105*, 7037−7047.
(33) Rauhut, G.; Pulay, P. Transferable Scaling Factors for Density Functional Derived Vibrational Force Fields. *J. Phys. Chem.* **1995**, *99*, 3093−3100.
(34) Califano, S. *Vibrational States*; Wiley: London, 1976.
(35) Papoušek, D.; Aliev, M. R. *Molecular Vibrational/Rotational Spectra*; Academia: Prague, Czech Republic, 1982.

(36) Nielsen, H. H. The Vibration−Rotation Energies of Molecules. *Rev. Mod. Phys.* **1951**, *23*, 90−136.
(37) Mills, I. M. Vibration−Rotation Structure in Asymmetric- and Symmetric-Top Molecules. In *Molecular Spectroscopy: Modern Research*; Rao, K. N., Matthews, C. W., Eds.; Academic Press: New York, 1972.
(38) Aliev, M. R.; Watson, J. K. G. Higher−Order Effects in the Vibration−Rotation Spectra of Semi-rigid Molecules. In *Molecular Spectroscopy: Modern Research*' Rao, K. N., Ed.; Academic Press: New York, 1985; Vol. *III*.
(39) Clabo, D. A., Jr.; Allen, W. D.; Remington, R. B.; Yamaguchi, Y.; Schaefer, H. F., III. A Systematic Study of Molecular Anharmonicity and Vibration−Rotation Interaction by Self-Consistent-Field Higher-Derivative Methods. Asymmetric Top Molecules. *Chem. Phys.* **1988**, *123*, 187−239.
(40) Sarka, K.; Demaison, J. Perturbation Theory, Effective Hamiltonians and Force Constants. In *Computational Molecular Spectroscopy*; Jensen, P., Bunker, P. R., Eds.; John Wiley & Sons Ltd.: New York, 2000.
(41) Barone, V. Anharmonic Vibrational Properties by a Fully Automated Second-Order Perturbative Approach. *J. Chem. Phys.* **2005**, *122*, 014108.
(42) Krasnoshchekov, S. V.; Stepanov, N. F. Anharmonic Force Fields and Perturbation Theory in the Interpretation of Vibrational Spectra of Polyatomic Molecules. *Russ. J. Phys. Chem. A* **2008**, *82*, 592−602.
(43) Krasnoshchekov, S. V.; Isayeva, E. V.; Stepanov, N. F. Numerical-Analytic Implementation of the Higher-Order Canonical Van Vleck Perturbation Theory for the Interpretation of Medium-Sized Molecule Vibrational Spectra. *J. Phys. Chem. A* **2012**, *116*, 3691−3709.
(44) Carbonniere, P.; Lucca, T.; Pouchan, C.; Rega, N.; Barone, V. Vibrational Computations Beyond the Harmonic Approximation: Performances of the B3LYP Density Functional for Semirigid Molecules. *J. Comput. Chem.* **2005**, *26*, 384−388.
(45) Krasnoshchekov, S. V.; Nechayev, V. V.; Isayeva, E. V.; Stepanov, N. F. Calculation of Anharmonic Intensities in Vibrational Spectra of Raman Scattering and Full Interpretation of the Vibrational Spectrum of *trans*-1,3-Butadiene. *Moscow Univ. Chem. Bull.* **2010**, *65*, 19−29.
(46) Martin, J. M. L.; Lee, T. J.; Taylor, P. R.; Francois, J.-P. The Anharmonic Force Field of Ethylene, C_2H_2, by Means of Accurate *Ab Initio* Calculations. *J. Chem. Phys.* **1995**, *103*, 2589−2602.
(47) Martin, J. M. L.; Taylor, P. R. Accurate Ab Initio Quartic Force Field for trans-HNNH and Treatment of Resonance Polyads. *Spectrochim Acta, Part A* **1997**, *53*, 1039−1050.
(48) Hänninen, V.; Halonen, L. Calculation of Spectroscopic Parameters and Vibrational Overtones of Methanol. *Mol. Phys.* **2003**, *101*, 2907−2916.
(49) Matthews, D. A.; Vásquez, J.; Stanton, J. F. Calculated Stretching Overtone Levels and Darling−Dennison Resonances in Water: A Triumph of Simple Theoretical Approach. *Mol. Phys.* **2007**, *105*, 2659−2666.
(50) Rosnik, A. M.; Polik, W. F. VPT2+K Spectroscopic Constants and Matrix Elements of the Transformed Vibrational Hamiltonian of a Polyatomic Molecule with Resonances Using Van Vleck Perturbation Theory. *Mol. Phys.* **2014**, *112*, 261−300.
(51) Secroun, C.; Barbe, A.; Jouve, P. Higher-Order Vibrational Intensities of Polyatomic Molecules. *J. Mol. Spectrosc.* **1973**, *45*, 1−9.
(52) Geerlings, P.; Berckmans, D.; Figeys, H. P. The Influence of Electrical and Mechanical Anharmonicity on the Vibrational Transition Moments of Diatomic and Polyatomic Molecules. *J. Mol. Struct.* **1979**, *57*, 283−297.
(53) Berckmans, D.; Figeys, H. P.; Geerlings, P. Contact Transformational and Quantum Chemical Calculations of the Integrated Intensities of Fundamental, First and Second Overtone, Binary Combination and Difference Infrared Absorption Bands of the Water Molecule. *J. Mol. Struct.: THEOCHEM* **1986**, *148*, 81−100.
(54) Willetts, A.; Handy, N. C.; Green, W. H., Jr.; Jayatilaka, D. Anharmonic Corrections to Vibrational Transition Intensities. *J. Phys. Chem.* **1990**, *94*, 5608−5616.
(55) Green, W. H.; Willetts, A.; Jayatilaka, D.; Handy, N. C. Ab Initio Prediction of Fundamental, Overtone and Combination Band Infrared Intensities. *Chem. Phys. Lett.* **1990**, *169*, 127−137.
(56) Polavarapu, P. L. Vibrational Optical Activity of Anharmonic Oscillator. *Mol. Phys.* **1996**, *89*, 1503−1510.
(57) Vásquez, J.; Stanton, J. F. Simple(r) Algebraic Equations for Transition Moments of Fundamental Transitions in Vibrational Second-Order Perturbation Theory. *Mol. Phys.* **2006**, *104*, 377−388.
(58) Barone, V.; Bloino, J.; Guido, C. A.; Lipparini, F. A Fully Automated Implementation of VPT2 Infrared Intensities. *Chem. Phys. Lett.* **2010**, *496*, 157−161.
(59) Bloino, J.; Barone, V. A Second-Order Perturbation Theory Route to Vibrational Averages and Transition Properties of Molecules: General Formulation and Application to Infrared and Vibrational Circular Dichroism Spectroscopies. *J. Chem. Phys.* **2012**, *136*, 124108.
(60) Barone, V.; Biczysko, M.; Bloino, J. Fully Anharmonic IR and Raman Spectra of Medium-Size Molecular Systems: Accuracy and Interpretation. *Phys. Chem. Chem. Phys.* **2014**, *16*, 1759−1787.
(61) Montero, S. Anharmonic Raman Intensities of Overtone, Combination and Difference Bands. *J. Chem. Phys.* **1982**, *77*, 23−29.
(62) Montero, S. Raman Intensities of Fermi Diads. I. Overtones in Resonance with Nondegenerate Fundamentals. *J. Chem. Phys.* **1983**, *79*, 4091−4100.
(63) Vidal, L. N.; Vazquez, P. A. M. CCSD Study of Anharmonic Raman Cross Sections of Fundamental, Overtone, and Combination Transitions. *Int. J. Quantum Chem.* **2012**, *112*, 3205−3215.
(64) Hanson, H.; Nielsen, H. H.; Schafer, W. H.; Waggoner, J. Intensities of Rotation Lines in Absorption Bands. *J. Chem. Phys.* **1957**, *27*, 40−43.
(65) Legay, F. Intensite Des Raies d'Une Bande de Vibration−Rotation. *Cah. Phys.* **1958**, *12*, 416−436.
(66) Long, D. A. *The Raman Effect: A Unified Treatment of The Theory of Raman Scattering by Molecules*; Wiley: Chichester, U.K., 2002.
(67) Frisch, M. J.; Trucks, G. W.; Schlegel, H. B.; Scuseria, G. E.; Robb, M. A.; Cheeseman, J. R.; Scalmani, G.; Barone, V.; Mennucci, B.; Petersson, G. A.; et al. *Gaussian 09*, revision B.01; Gaussian, Inc.: Wallingford, CT, 2010.
(68) Fogarasi, G.; Zhou, X.; Taylor, P. W.; Pulay, P. The Calculation of Ab Initio Molecular Geometries: Effect Optimization by Natural Internal Coordinates and Empirical Correction by Offset Forces. *J. Am. Chem. Soc.* **1992**, *114*, 8191−8201.
(69) Xie, Y.; Fan, K.; Boggs, J. E. The Harmonic Force Field and Vibrational Spectra of Pyrrole. *Mol. Phys.* **1986**, *58*, 401−411.
(70) Krasnoshchiokov, S. V.; Abramenkov, A. V.; Panchenko, Y. N.; Matveev, V. K.; Pentin, Y. A. Finding of Redundant Coordinates and Coefficients of Linear-Dependence in a System of Molecular Internal Valence Coordinates. *Vestn. Mosk. Univ., Ser. 2: Khim.* 1984, *25*, 357−361; in Russian.
(71) Krasnoshchekov, S. V.; Isayeva, E. V.; Stepanov, N. F. Criteria for First- and Second-Order Vibrational Resonances and Correct Evaluation of the Darling−Dennison Resonance Coefficients Using the Canonical Van Vleck Perturbation Theory. *J. Chem. Phys.* **2014**, submitted.
(72) Krasnoshchekov, S. V.; Craig, N. C.; Stepanov, N. F. Anharmonic Vibrational Analysis of the Gas-Phase Infrared Spectrum of 1,1-Difluoroethylene Using the Operator Van Vleck Canonical Perturbation Theory. *J. Phys. Chem. A* **2013**, *117*, 3041−3056.
(73) Martin, J. M. L.; El-Yazal, J.; François, J.-P. Basis Set Convergence and Performance of Density Functional Theory Including Exact Exchange Contributions for Geometries and Harmonic Frequencies. *Mol. Phys.* **1995**, *86*, 1437−1450.
(74) Boese, A. D.; Klopper, W.; Martin, J. M. L. Assessment of Various Density Functionals and Basis Sets for the Calculation of Molecular Anharmonic Force Fields. *Int. J. Quantum Chem.* **2005**, *104*, 830−845.

(75) Loboda, O.; Tunell, I.; Minaev, B.; Ågren, H. Theoretical Study of Triplet State Properties of Free-Base Porphin. *Chem. Phys.* **2005**, *312*, 299−309.